Development 133, 4281-4292 (2006) doi:10.1242/dev.02615

The puromycin-sensitive aminopeptidase PAM-1 is required for meiotic exit and anteroposterior polarity in the one-cell *Caenorhabditis elegans* embryo

Rebecca Lyczak[1,2,*], Lynnsey Zweier[1], Thomas Group[1], Mary Ann Murrow[1], Christine Snyder[1], Lindsay Kulovitz[1], Alexander Beatty[1], Kristen Smith[1] and Bruce Bowerman[2]

In the nematode *Caenorhabditis elegans*, sperm entry into the oocyte triggers the completion of meiosis and the establishment of the embryonic anteroposterior (AP) axis. How the early embryo makes the transition from a meiotic to a mitotic zygote and coordinates cell cycle changes with axis formation remains unclear. We have discovered roles for the *C. elegans* puromycin-sensitive aminopeptidase PAM-1 in both cell cycle progression and AP axis formation, further implicating proteolytic regulation in these processes. *pam-1* mutant embryos exhibit a delay in exit from meiosis: thus, this peptidase is required for progression to mitotic interphase. In addition, the centrosomes associated with the sperm pronucleus fail to closely associate with the posterior cortex in *pam-1* mutants, and the AP axis is not specified. The meiotic exit and polarity defects are separable, as inactivation of the B-type cyclin CYB-3 in *pam-1* mutants rescues the meiotic exit delay but not the polarity defects. Thus PAM-1 may regulate CYB-3 during meiotic exit but presumably targets other protein(s) to regulate polarity. We also show that the *pam-1* gene is expressed both maternally and paternally, providing additional evidence that sperm-donated gene products have important roles during early embryogenesis in *C. elegans*. The degradation of proteins through ubiquitin-mediated proteolysis has been previously shown to regulate the cell cycle and AP axis formation in the *C. elegans* zygote. Our analysis of PAM-1 requirements shows that a puromycin-sensitive aminopeptidase is also required for proteolytic regulation of the oocyte to embryo transition.

KEY WORDS: *C. elegans*, Anteroposterior axis, Meiotic exit, PAM-1, CYB-3, Aminopeptidase

INTRODUCTION

In *Caenorhabditis elegans*, sperm entry into the oocyte triggers the completion of meiosis. Before oocyte maturation, the oocyte chromosomes are arrested at diakinesis of meiosis I (Greenstein, 2005). Maturation cues entry into metaphase I (Greenstein, 2005), but fertilization is required for extrusion of the first polar body and the second meiotic division (McNally and McNally, 2005). During meiosis, the sperm chromosomes remain condensed near the future posterior pole. Immediately following extrusion of the second polar body, the embryo exits meiosis, the sperm and egg chromosomes decondense, and pronuclei appear as the embryo enters the first mitotic interphase (Albertson and Thomson, 1993; Schneider and Bowerman, 2003).

Near the end of meiosis II or during the first interphase, the anteroposterior (AP) axis is established. During axis formation, the sperm pronucleus/centrosome complex (SPCC) is closely apposed to the cell membrane at the cortex of the zygote (Rappleye et al., 2002), and its position defines the posterior pole (Albertson, 1984; Goldstein and Hird, 1996; Schneider and Bowerman, 2003). Evidence points to the centrosome as the key SPCC component that orchestrates axis polarization (Cowan and Hyman, 2004b; Hamill et al., 2002; O'Connell et al., 2000; Sadler and Shakes, 2000; Sonneville and Gönczy, 2004). The centrosome, by an unknown mechanism, appears to destabilize the cortical actomyosin network in the posterior (Munro et al., 2004). This destabilization results in a flow of cortical F-actin and nonmuscle myosin to the anterior pole, along with the PDZ-domain polarity proteins PAR-3 and PAR-6 (Cuenca et al., 2003; Munro et al., 2004). Following this initial polarization, the ring-finger protein PAR-2 becomes enriched at the posterior cortex, where it stabilizes polarity (Cuenca et al., 2003; Munro et al., 2004). These reciprocal domains are then maintained due to interactions between the PAR proteins themselves (Cuenca et al., 2003). The PAR proteins are required for all but the initial AP asymmetries, which occur in response to the centrosome, including posterior displacement of the first mitotic spindle and the polarized distribution of the germline P granules and developmental determinants (Cowan and Hyman, 2004a; Lyczak et al., 2002; Schneider and Bowerman, 2003).

One process that is important for axis formation is cell cycle progression, as polarity establishment occurs immediately after meiotic exit. Moreover, many mutants with meiotic defects also have polarity defects, although these are in some cases separable (Liu et al., 2004; Rappleye et al., 2002; Shakes et al., 2003; Sonneville and Gönczy, 2004). For example, the scaffolding protein CUL-2 and its putative adaptor ZYG-11 are components of a cullin-based E3 ligase required for progression through meiosis and AP axis formation, most likely through degradation of different targets (Liu et al., 2004; Sonneville and Gönczy, 2004). Nevertheless, proper progression through meiosis may be important for axis formation. Mutants with a partial loss of the anaphase-promoting complex (APC) sometimes completely bypass meiosis II, and when this bypass occurs these mutants exhibit AP axis defects (Shakes et al., 2003). These results suggest that either cell cycle progression is important for AP polarity establishment, or that the machineries governing cell cycle progression and cell polarity share some components.

If common machinery links meiotic completion and axis establishment, it may be proteolytic. All the proteins mentioned above are components of either the APC or SCF E3 ubiquitin ligase

[1]Department of Biology, Ursinus College, Collegeville, PA 19426, USA. [2]Institute of Molecular Biology, University of Oregon, Eugene, OR 97403, USA.

*Author for correspondence (e-mail: rlyczak@ursinus.edu)

Accepted 6 September 2006

complexes, proposed to target specific substrates for degradation during the cell cycle (Bowerman and Kurz, 2006; Koepp et al., 1999). Furthermore, CUL-2-based ECS E3 ligase(s) have been shown to regulate cell polarity by degrading developmental determinants in the anterior or posterior cytoplasm during and after the first asymmetric division of the one-cell zygote (DeRenzo et al., 2003). Acting downstream of these E3 ubiquitin ligases is the 26S proteasome. Intriguingly, a puromycin-sensitive aminopeptidase (PSA) appears to colocalize with the 26S proteosome and to participate in proteolytic events to regulate the cell cycle in mammalian cells (Constam et al., 1995). PSA family members are metalloproteases that hydolyze N-terminal amino acids and are members of the M1 metalloprotease family, characterized by the $HEXXH(X)_{18}E$ metal coordination site and an upstream GAMEN motif (Laustsen et al., 2001). These peptidases are widely conserved and include a human family member (Taylor, 1993). *Caenorhabditis elegans* has one PSA homolog, PAM-1, a cytoplasmic aminopeptidase localized to neurons and intestinal cells in larvae and adults (Brooks et al., 2003). While PSA has been implicated in cell cycle regulation in mammals, its requirements remain largely unstudied. Here we show that *C. elegans* PAM-1 is contributed by both the sperm and the egg, and is required for timely exit from meiosis and AP axis specification. These two processes appear to be independently regulated by PAM-1. We propose that PAM-1 is part of proteolytic machinery in the early embryo used to trigger meiotic completion and trigger axis formation through regulated protein degradation.

MATERIALS AND METHODS

Strains and nematode culture

Caenorhabditis elegans were cultured as described (Brenner, 1974). N2 Bristol was used for wild-type and CB4856 for SNP mapping. The following alleles and balancers were used: LG I *dpy-5(e61)*; LG II *rol-6(e187)*; LG III *unc-32(e189)*; LG IV *unc-5(e53)*, *bli-6(sc16)*, *unc-8(e49)*, *pam-1(or282ts)*, *pam-1(or403ts)*, *pam-1(or347ts)*, *pam-1(or547ts)*, *pam-1(or370ts)*, *unc-24(e138)*, *dpy-20(e1282)*, *him-8(e1489)*, DnT1 (LG IV/V translocation balancer); LGV *him-5(e1409)*, *dpy-11(e224)*, *fog-2(q71)*, *unc-51(e1189)*; *X lon-2(e678)*.

GFP lines: JH227 *pie-1::*GPF axEx73[pJH3.92;pRF4] (Reese et al., 2000); WH204 *pie-1::*GFP::β-TUBULIN (Strome et al., 2001); and AZ212 *pie-1*::GFP::H2B (Praitis et al., 2001) were used to construct strains EU929 *pam-1(or282ts)/DnT1* IV; *+/DnT1* V; *pie-1::GFP* axEx73[pJH3.92;pRF4], EU881 *pam-1(or282ts)* IV; *pie-1*::GFP::β-TUBULIN, and EU947 *pam-1(or282ts)/DnT1* IV; *+/DnT1* V; *pie-1*::GFP::H2B. The CYB-3::GFP strain was provided by P. Gönczy (Sonneville and Gönczy, 2004).

Homozygous temperature-sensitive strains were propagated at the permissive temperature of 15°C. L4 larvae were shifted to 25°C overnight before analysis of the mutant embryos.

Isolation and characterization of *pam-1* alleles

Five *pam-1* alleles (*or282ts, or347ts, or370ts, or403ts, or547ts*) were identified in a screen for temperature-sensitive embryonic lethal mutants (Encalada et al., 2000). This locus was originally named *scu-1* (sperm cue abnormal) but subsequently changed to *pam-1* after gene identity was determined. Complementation tests were performed for each allele with *or282ts*. All alleles showed weak temperature sensitivity for embryonic lethality when homozygous hermaphrodites were shifted to 25°C as L4s. *pam-1(or282ts)* was 85.3% embryonic lethal at 15°C (*n*=495), and 97.0% embryonic lethal at 25°C (*n*=396). Similarly, *pam-1(or403ts)* was 88.7% embryonic lethal at 15°C (*n*=1029), and 98.5% embryonic lethal at 25°C (*n*=470). All phenotypic characterization was performed with these two alleles.

To test for a zygotic requirement, hermaphrodites of strain *pam-1(or282ts) unc-24(e138)/+* or *pam-1(or403)/dpy-13(e184) unc-24(e138)* were allowed to make embryos at 25°C: nearly all embryos hatched (705/716; 425/428, respectively). To test for paternal requirements, *fog-2* females from strain CB4108 were mated at 25°C with EU983 *pam-1(or403); him-5* mutant males, which had been raised at 25°C from the L1 stage. To test for maternal requirements, *pam-1(or403)*; *unc-51 fog-2* females were crossed with N2 males at 25°C. From each cross, females were removed after mating for embryo analysis. As a control, CB4108 *fog-2* females were crossed with N2 males.

For deficiency analysis, *pam-1(or282ts)* males were mated into hermaphrodites from the following strains: RW1324 *fem-1(e1991) unc-24(e138) unc-22(s12)/stDf7* IV and RW1333 *fem-1(e1991) unc-24(e138) unc-22(s12)/stDf8* IV at the permissive temperature. F1 animals were shifted to 25°C and embryos from *pam-1(or282ts)/stDf7* (*n*=3) or *pam-1(or282ts)/stDf8* (*n*=3) worms were imaged using DIC microscopy.

Positional cloning

Linkage group and 3-factor mapping (Brenner, 1974) were used to position the *or282ts* allele to +3.39 on chromosome IV. Single nucleotide polymorphism (SNP) mapping (Wicks et al., 2001) was then done using SNPs identified from The University of Washington Genetics and Genome Sequencing Center. Unc-nonPam recombinants were found from strains heterozygous for CB4856 DNA and either *unc-8(e49) pam-1(or282)* or *pam-1(or282) unc-24(e138)*. PCR-amplified DNA was isolated from recombinants using a kit from Gentra Systems and scored for the SNPs to narrow the region to between cosmids R05G6 and C06A6.

The entire coding region of candidate genes in the region were sequenced directly from PCR products produced from purified DNA for each allele. For each sequencing reaction, four independent PCR reactions were combined and purified using the QUIAquick PCR purification kit (Quiagen) and sequenced at the Nucleic Acid/Protein Research Core Facility at the Children's Hospital of Philadelphia. Sequences and chromatograms were aligned and compared to the published sequence using DNASIS MAX software (Hitachi). All potential sequences were confirmed via a secondary PCR and sequencing reaction. The *pam-1* gene was amplified in two separate reactions using primers f49e8.3a: CAAAATTGACGAGAGGGG with f49e8.3b: GTGATCCAGGAGTCACG and f49e8.3c: GCCAAAGA-TCAGTCCACC with f49e8.3d: AAGCAAGATGATGCCACG.

Mutations found in all five alleles are detailed below. Nucleotide numbers are based on position in the confirmed sequence for F49E8.3a. In *or370*, a G to A substitution was found at nucleotide 1022 and resulted in an A278T change. In *or347*, a C to T substitution was at nucleotide 1023 and resulted in A278W. In *or403* a G to A change was observed at nucleotide 1849 and resulted in W538X. In *or547* a C to T substitution at nucleotide 2027 was observed, which resulted in Q598X. In *or282* a deletion from nucleotide 283 to 873 was found in the genomic DNA. This deletion resulted in an amino acid sequence change following K56 to NNFSX.

Microscopy and immunoflorescence

For time-lapse imaging, embryos were placed on a 3% agarose cushion under a coverslip. DIC images were captured every 5 seconds using a Dage MT1 VE1000 camera and Scion Image software, or Nikon Eclipse E600 and SPOT Basic software. Cortical flows were time-lapsed as previously described (Severson et al., 2002). PIE-1::GFP and TUBULIN::GFP images were acquired using epifluorescence and a Micromax EBF512 cooled CCD camera (Roper Scientific) under the control of Metamorph imaging software (Universal Imaging). HISTONE::GFP images were captured similarly except on a spinning disk confocal (Perkin Elmer) or a Nikon C1 Confocal Imaging System. For time-lapse GFP imaging, a Z-series of 5-15 frames was acquired at 1.5 μm intervals every 20-60 seconds and in some experiments one center-plane DIC image was captured. Imaging of meiosis was performed in utero with worms anesthetized in 0.1% tricane and 0.01% tetramisole (McCarter et al., 1999). Measurements of pronuclear meeting position and centrosome movements were made using Object-Image software.

The following primary antibodies and dilutions were used: rabbit anti-PAR-2 (1:5), rabbit anti-PAR-3 (1:20), both a gift from K. Kemphues, rabbit anti-PGL-1 (1:10,000), a gift from S. Strome, mouse anti-tubulin (1:250) (Sigma clone DM 1A), and mouse anti-actin (1:200) (ICN clone C4). Immunostaining was done using a methanol fix protocol (Severson et al.,

2002). The DNA was stained with 0.2 μm TOTO3 (Molecular Probes) or DAPI in Antifade mounting media (Invitrogen). Embryos were imaged on a BioRad MRC 1024 laser scanning confocal microscope or a Nikon C1 confocal microscope system.

RNA interference

Feeding RNAi was used to inactivate *cyb-3* as described (Kamath et al., 2003). Bacteria were grown on plates containing 1 mmol/l IPTG and 75 μg/μl carbenacillin and placed at 37°C overnight. L4 worms were picked to the plates and grown at 25°C for 24 hours before analysis.

RESULTS

Identification of mutations in the *pam-1* gene

In a screen for maternal-effect embryonic lethal mutants, we identified five partially conditional recessive alleles of a gene we determined to be *pam-1* (puromycin-sensitive aminopeptidase; see below). Our phenotypic analysis was performed with two alleles, *pam-1(or282ts)* and *pam-1(or403ts)*. Unless the allele is specified, we refer hereafter to embryos produced by homozygous *pam-1(or282* or *or403)* mutant hermaphrodites raised at the restrictive temperature as *pam-1* mutants.

To identify the molecular lesion in *pam-1* mutants, the gene was mapped to a small interval (see Materials and methods). We sequenced candidate genes in the region and found, in all five mutant alleles, mutations in the puromycin-sensitive aminopeptidase gene called *pam-1* (Fig. 1). This gene is closely related to mouse and human PSA genes (Fig. 1). Two of the alleles contained missense mutations. The A278T mutation in *pam-1(or370)* and the A278V mutation in *pam-1(or347)* both altered the GAMEN motif that is conserved in all M1 aminopeptidases and has been shown in other systems to be important for full enzyme activity (Laustsen et al., 2001). Two of the alleles encoded nonsense mutations. Both the W538X mutation in *pam-1(or403)* and the Q598X mutation in *pam-1(or547)* are predicted to truncate the protein downstream of the active site (Fig. 1). A 590 bp deletion was found in *pam-1(or282)*, resulting in a change following K56 to NNFSX and thus a truncated protein product. All five alleles are recessive and *pam-1(or282)* is most likely a null, as this deletion results in a frameshift and stop codon before the active site. Additionally, embryos produced by hemizygous mothers (with one mutant copy of *pam-1* in trans to a chromosomal deficiency that removes *pam-1*) were indistinguishable from those produced by homozygous *pam-1(or282)* mothers (data not shown).

pam-1 embryos exhibit a meiotic exit defect

The first defects observed in *pam-1* mutant embryos occurred during meiosis. The timing of meiosis was compared in wild-type and *pam-1* embryos in utero using a HISTONE::GFP line (H2B::GFP) to fluorescently label chromosomes in live embryos (Table 1). We detected no significant difference in the timing of completion of either meiosis I or II in *pam-1(or282)* mutants, compared to wild-type embryos. For these experiments we defined the end of meiosis as the time when polar body extrusion was evident. However, we did observe meiosis II defects in 33% (4/12) of *pam-1(or282)* embryos. In these embryos, a DNA bridge connected the separating anaphase chromosomes (Fig. 2B).

In contrast to the incomplete penetrance of the meiotic chromosome segregation defects, all *pam-1(or282)* embryos exhibited a significant delay in exiting meiosis II. Here we define meiotic exit as the time between extrusion of the second polar body and the appearance of pronuclei as detected using differential interference contrast (DIC) microscopy. Shortly after extrusion of the second polar body in wild type, both the oocyte and sperm chromosomes began to decondense, and pronuclei became evident (Fig. 2A, parts a-c; Table 1). However, in *pam-1* mutants the chromosomes remained condensed after polar body extrusion, and oocyte and sperm pronuclear envelope formation was delayed (Fig. 2A, parts d-f). In wild-type embryos pronuclei were detectable on average 3.39 minutes after polar body extrusion, but in *pam-1* mutant embryos, pronuclei were visible after an average of 16.86 minutes (Table 1). In some cases, the oocyte pronucleus never became visible using DIC optics (4/17; data not shown). These severe delays indicate that *pam-1* mutant embryos are defective in the regulation or execution of meiotic exit.

Meiotic exit defects are rescued by loss of cyclin B3

Previous studies have shown that inactivation of B-type cyclins is necessary for exit from meiosis in several organisms. For example, reduction of the cyclin encoded by *cyb-3* in *C. elegans* has been shown to rescue meiotic exit delays in *zyg-11* mutants (Sonneville and Gönczy, 2004). We therefore asked if *cyb-3* was required for the meiotic exit delay in *pam-1* mutants, using RNAi to deplete CYB-3. As previously shown (Sonneville and Gönczy, 2004), we found that *cyb-3(RNAi)* embryos exhibit a prolonged meiosis II, but a timely exit from meiosis (Table 1). In *pam-1(or282); cyb-3(RNAi)* embryos that completed meiosis II and extruded a second polar body, we observed a marked decrease in the time of meiotic exit, similar to wild type (Table 1). Thus depletion of CYB-3 rescues the meiotic exit defect in *pam-1* mutants, suggesting that PAM-1 may promote CYB-3 degradation to permit exit from meiosis.

Interestingly, in some *pam-1(or282);cyb-3(RNAi)* embryos, a second polar body was never extruded. Embryos entered into metaphase II, but never progressed into a clear anaphase stage before chromosome decondensation became evident. In these embryos, the timing from meiosis II to appearance of the pronuclei appeared to be lengthened even over *cyb-3(RNAi)* alone (Table 1), suggesting a possible role for PAM-1 in meiosis II.

pam-1 embryos lack early signs of AP polarity

Because polarity defects are associated with meiotic progression defects in other *C. elegans* mutants, we next examined AP axis formation in *pam-1* mutant and wild-type embryos using DIC optics. As the SPCC contacts the posterior cortex and polarizes the AP axis in wild type, cortical changes are apparent in which the posterior cortex smoothens and the anterior cortex ruffles while cortical flows occur (Fig. 3A). The oocyte pronucleus then migrates to meet the sperm pronucleus in the posterior (Fig. 3B). Together the pronuclei and associated centrosomes move to the center of the embryo and set up the first mitotic spindle, which displaces posteriorly during anaphase, resulting in an asymmetric division (Fig. 3C,D). The two daughters differ in size, cell-cycle timing and spindle orientation (Fig. 3E) (Hyman and White, 1987; Sulston et al., 1983).

pam-1 mutant embryos failed to exhibit the earliest signs of AP axis polarization. In most embryos the SPCC failed to make a tight association with the cortex (54/60) and was often near the center of the embryo when it first became visible (46/60; Fig. 3F). In addition, SPCC-cued polarity was not apparent. The cortex did not smoothen at either pole, membrane ruffling persisted around the entire periphery, and a pseudocleavage furrow failed to form (54/60; Fig.

3F). Furthermore, cortical flows were absent (*n*=6; data not shown). Thus it seems that the cortex did not polarize in *pam-1* mutant embryos.

pam-1 mutant embryos also lacked polarity downstream of the initial sperm cue. Based on time-lapse DIC analysis, the pronuclei met closer to the center of the embryo (Fig. 3G,K) and the first mitotic spindle was often mis-positioned. Posterior placement of the spindle was observed in all embryos that exhibited normal SPCC cortical association (6/6). However, in embryos lacking SPCC association, most divided symmetrically (32/54; Fig. 3H,I), but surprisingly some divided asymmetrically with the spindle oriented either toward the posterior (17/54) or toward the anterior (5/54). When *pam-1* mutant embryos divided asymmetrically, the daughter cells exhibited further asymmetries, as in wild-type embryos (data

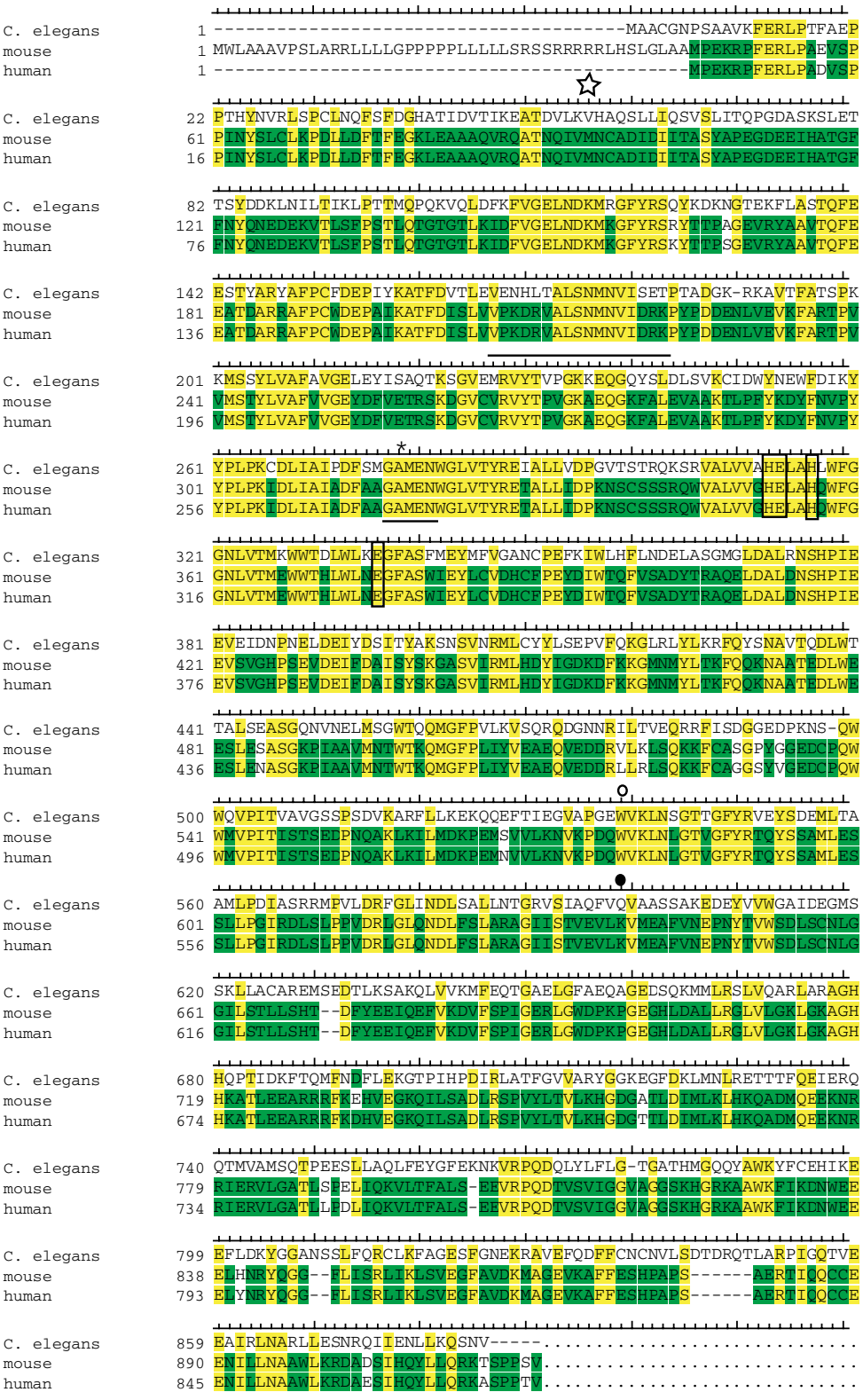

Fig. 1. *pam-1* encodes a puromycin-sensitive aminopeptidase. Alignment of PAM-1 amino acid sequence showing conservation with mouse (GenBank AAH86798) and human (GenBank NP_006301) PSA (see also Brooks et al., 2003). Colored blocks mark amino acid identity. Overlined area denotes region of homology with 26S proteasome subunits (Constam et al., 1995). The underlined GAMEN motif is characteristic of M1 family metalloproteases and the site of two of the missense mutations A278W in *pam-1(or347)* and A278T in *pam-1(or370)* (marked with *). The boxed amino acids in the HEXXH(X)$_{18}$E motif are necessary for zinc binding. The star denotes the site of deletion in *pam-1(or282)*. The open circle denotes the position of the stop codon present in *pam-1(or403),* W538X, while the closed circle denotes the position of the stop codon present in *pam-1(or547)*, Q598X.

Table 1. Meiotic timing in *pam-1* and *pam-1; cyb-3(RNAi)* embryos

	Minutes in each phase of meiosis		
Genotype	Meiosis I	Meiosis II	Meiotic exit
N2	13.81±1.24, *n*=9	12.43±3.01, *n*=9	3.39±1.93, *n*=9
pam-1	13.73±2.35, *n*=5	14.80±3.03, *n*=5	16.83±7.42, *n*=5
cyb-3(RNAi)	18.36±5.82, *n*=6	29.30±12.91, *n*=5	1.94±0.33, *n*=5
pam-1;cyb-3(RNAi)	17.91±2.73, *n*=10	22.10±3.19, *n*=5	3.05±1.37, *n*=5
		*45.39±12.97, *n*=5	

Meiosis I, oocyte entry into the spermatheca to extrusion of the first polar body; meiosis II, time between extrusion of the first and second polar bodies; meiotic exit, time between extrusion of the second polar body and appearance of the pronuclei via DIC optics.
*Embryos that failed to extrude a second polar body and are timed from extrusion of first polar body to pronuclear appearance.

not shown). However, when *pam-1* embryos divided symmetrically, both daughters divided synchronously with parallel spindles transverse to the AP axis (Fig. 3J). We conclude that signs of SPCC cortical association and cortical polarity are absent in most *pam-1* mutant embryos, and that this results in a symmetric division in a just over half of all embryos.

pam-1 is required for localization of polarity determinants

Because most *pam-1* mutant embryos lacked early signs of polarity, we next used indirect immunofluorescent labeling of fixed embryos to examine the localization of the cortical polarity regulators called the PAR proteins. As expected, in wild-type one-cell embryos, PAR-2 and PAR-3 localized to the cortex in reciprocal domains, with PAR-2 in the posterior and PAR-3 in the anterior (Table 2; Fig. 4A,D) (Rose and Kemphues, 1998). In one-cell *pam-1* mutant embryos we observed defects in the localization of both proteins (Table 2; Fig. 4B,C,E). PAR-2 was not detected at the cortex in 44.5% of *pam-1* mutant embryos (Table 2; Fig. 4B). In 60% of embryos with detectable PAR-2 at the cortex, it was mislocalized to a small lateral patch, which did not correlate with meiotic spindle position or polar body location (Table 2; Fig. 4C). In about 56% of *pam-1* mutant embryos, PAR-2 was detected in puncta near the centrosomes and their asters (Fig. 4B). While this peri-centrosome staining occurred most frequently in embryos lacking cortical PAR-2, it was also observed in embryos in which cortical PAR-2 was mislocalized or properly localized. Only 20% of one-cell *pam-1* mutant embryos showed normal cortical PAR-2 staining restricted to the posterior pole. As a control, cortical actin localization appeared normal in these embryos, despite the loss of PAR-2 at the cortex (*n*=10; data not shown). In contrast to the loss of PAR-2 at the cortex, PAR-3 was distributed throughout the cortex in most *pam-1* mutant embryos (Table 2; Fig. 4E). Thus in most *pam-1* mutant embryos, the initial polarization that normally restricts PAR-3 to the anterior pole appears to be defective.

pam-1 is required for the localization of cell fate determinants

Next we examined the localization of cytoplasmic determinants that are normally restricted to the posterior pole of the embryo during the first mitotic division (Fig. 4F-I). In wild-type embryos the germline P granules are found throughout the cytoplasm during meiosis but

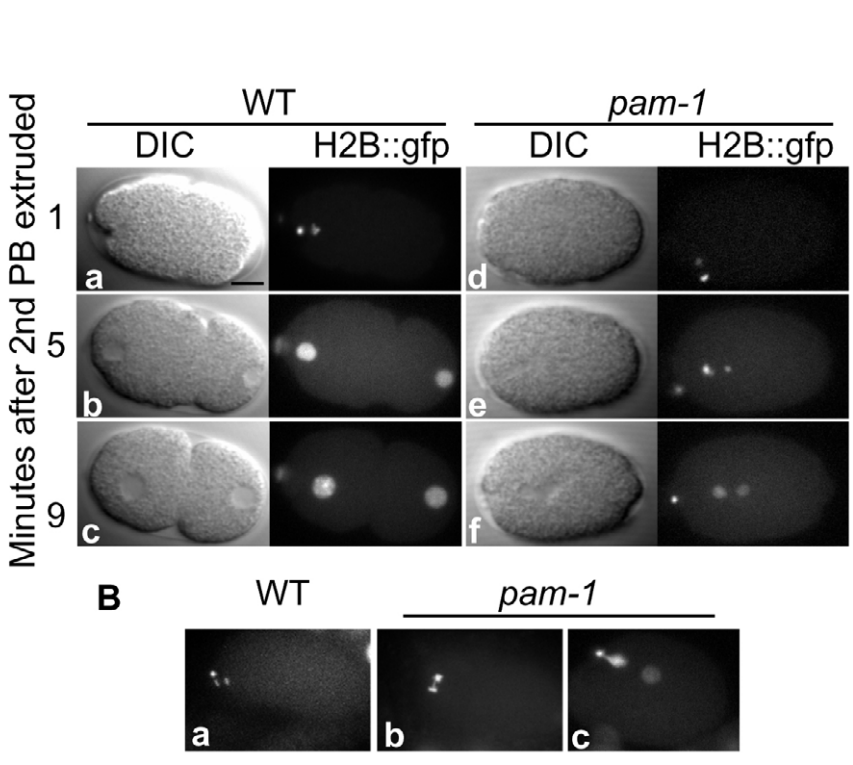

Fig. 2. Meiotic defects in *pam-1*. (**A**) Time-lapse images of embryos from H2B::GFP strains. (A, parts a-c) In wild type, the pronuclei were apparent by DIC optics, within a few minutes of meiotic completion. (A, parts d-f) By contrast, the time of pronuclear appearance in *pam-1* was significantly delayed. The condensed sperm chromosomes moved toward the oocyte chromosomes before the pronuclear envelopes formed. (**B**, part a) In wild type, chromosome segregation was clearly visible at the anterior cortex during meiosis II. (B, part b) In some *pam-1* embryos, a DNA bridge was observed between the separating chromosomes in meiosis II. (B, part c) In some embryos this bridge persisted and the oocyte pronucleus and second polar body remained joined. Scale bar: 10 μm.

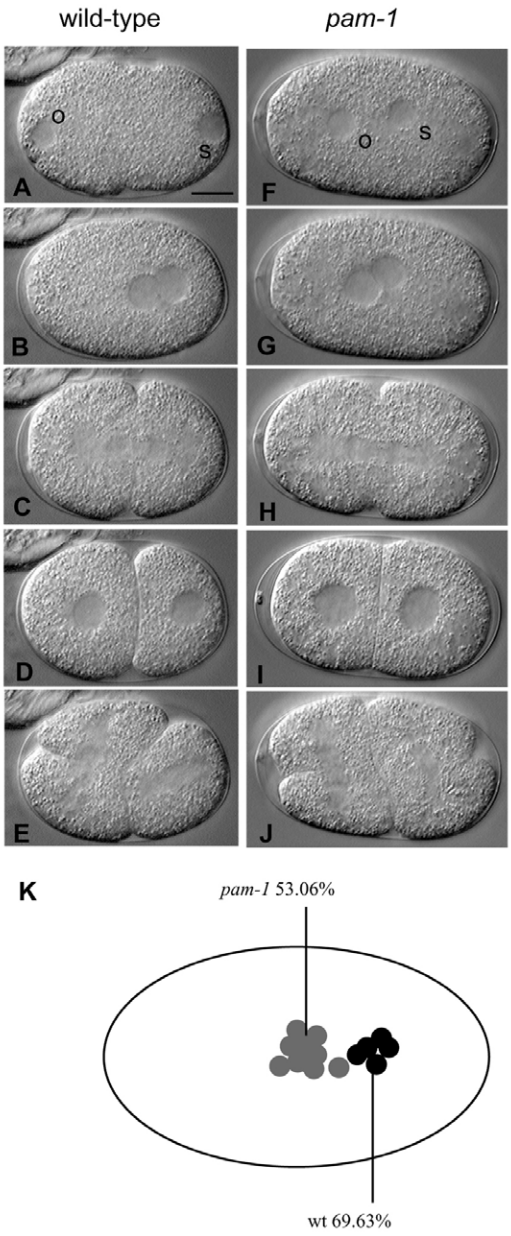

Fig. 3. *pam-1* embryos lack early signs of AP polarity. Images from a time-lapse DIC series of a single embryo. (**A**) In wild type, the oocyte and sperm pronuclei appeared at opposite ends of the embryo, with the sperm pronucleus at the posterior pole. The SPCC cued axis polarization and caused changes in the cortex called pseudocleavage. (**B**) The oocyte pronucleus migrated to meet the sperm pronucleus in the posterior of the embryo. (**C**,**D**) The first spindle displaced toward the posterior and the first cleavage was asymmetric, with a larger anterior cell, AB, and a smaller posterior cell, P_1. (**E**) These cells then differed in their cell cycle timing and spindle orientations during the next division. (**F**) In *pam-1* embryos, polarization of the cortex was absent and the SPCC did not contact the posterior cortex as the pronuclei first appeared close to the center of the embryo. (**G**) The pronuclei met in the center of the cell. (**H**,**I**) In about 60% of *pam-1* embryos, the first mitotic spindle remained in the center of the embryo, resulting in an equivalent cleavage. (**J**) When this occurred, the two daughter cells divided synchronously with parallel spindle orientations. (**K**) The position of pronuclear meeting was plotted for five wild-type and ten *pam-1* embryos. On average, the pronuclei in *pam-1* embryos met closer to the center of the embryo than in wild type. o, oocyte pronucleus; s, sperm pronucleus. Scale bar: 10 μm.

then localize posteriorly before the first mitosis (Hird et al., 1996; Strome and Wood, 1982). Similarly, in fixed, wild-type embryos (n=19), we observed posterior localization in one-cell embryos and localization to the P_1 cell at the two-cell stage (Table 3; Fig. 4F,F′). By contrast, P granules were not localized to one pole in 67% of fixed *pam-1* mutant one-cell embryos and were also mislocalized in later stage embryos (Table 3; Fig. 4G,G′).

To see if proper determinant localization correlated with an asymmetric first cleavage, we followed localization of the cytoplasmic and nuclear transcription factor PIE-1 in live embryos expressing PIE-1 fused to green fluorescent protein (PIE-1::GFP). In wild-type embryos, PIE-1 is enriched in posterior cytoplasm before the completion of P_0 mitosis and segregated to the posterior daughter P_1 after the first mitosis (Fig. 4H,H′; n=3) (see Reese et al., 2000). By contrast, PIE-1::GFP was distributed throughout the cytoplasm in 41% of one-cell *pam-1* embryos (7/17; Fig. 4I). Of the embryos with mislocalized PIE-1::GFP, some divided asymmetrically (3/7) and others divided symmetrically (4/7) during the first mitosis. By contrast, the majority of embryos that properly segregated PIE-1::GFP went on to divide asymmetrically (data not shown; 7/10). By the late two-cell stage, most asymmetric embryos exhibited normal PIE-1::GFP localization (12/13), and all symmetric embryos showed diffuse mislocalized PIE-1::GFP (16/16; Fig. 4I). We conclude that PAM-1 is necessary to promote proper segregation of developmental determinants along the AP axis during the first mitotic division.

pam-1 polarity defects are separable from meiotic exit defects

As meiotic exit and axis polarization occur in rapid succession in the one-cell embryo, we asked if the polarity defects in *pam-1* mutants might be a secondary consequence of the meiotic exit defect. As described above, CYB-3/Cyclin B depletion rescued the meiotic exit defect in *pam-1* mutants. We next asked whether the AP polarity defects were also rescued in CYB-3-depleted *pam-1* mutant embryos. *pam-1; cyb-3(RNAI)* embryos were observed through the first cell division for signs of polarity, such as pseudocleavage and asymmetric spindle positioning. While all *cyb-3(RNAi)* embryos observed showed normal pseudocleavage and a posteriorly displaced spindle (n=7), many *pam-1; cyb-3(RNAi)* embryos lacked pseudocleavage (n=16/23) and had spindles positioned toward the anterior (n=5/20) or center (n=6/20) (Fig. 5A-D). As only some *pam-1; cyb-3(RNAi)* embryos exit meiosis promptly, due to meiosis II defects in others (see above), we examined whether embryos with rescued meiotic exit were additionally rescued for polarity. We saw no such correlation; *pam-1; cyb-3(RNAi)* embryos that promptly exited meiosis showed no signs of polarity 55% of the time (n=9). As an additional marker, we examined P granule localization in *cyb-3(RNAi)* and in *pam-1(or403); cyb-3(RNAi)* embryos (Table 3; Fig. 5). All *cyb-3(RNAi)* embryos examined showed normal posterior localization of the P granules during the first mitosis (Fig. 5E,G; Table 3) (see also Sonneville and Gönczy, 2004). By contrast, even though *pam-1(or282); cyb-3(RNAi)* embryos often exhibited meiotic exit timings similar to wild type (Table 1), P granule localization was still severely defective in many embryos (Fig. 5F-I; Table 3). As a control to determine if CYB-3 levels could be eliminated effectively by RNAi treatment, we exposed CYB-3::GFP-expressing worms (Sonneville and Gönczy, 2004) to *cyb-3* RNAi. While all untreated worms (n=6), displayed strong oocyte GFP expression, we detected no GFP in all treated worms (n=8),

Table 2. PAR-2 and PAR-3 localization in one-cell *pam-1* mutants

		% Embryos with PAR localization patterns in each category		
PAR-2	*n*	Posterior	No cortical localization	Lateral patch
N2	25	100%	0%	0%
pam-1	45	22.2% (1/10)	44.5% (16/20)	33.3% (8/15)
PAR-3	*n*	Anterior	Around whole periphery	
N2	24	100%	0%	
pam-1	17	35.3%	64.7%	

Parentheses represent the number of embryos in each class that also exhibit PAR-2 cytoplasmic puncta.

suggesting that incomplete elimination of CYB-3 does not account for the persistent polarity defects (data not shown). We conclude that the polarity defects in *pam-1* mutants occur even in the absence of meiotic exit defects.

Aberrant centrosome positioning in *pam-1* mutants

The abnormally late appearance of pronuclei and the central appearance of the pronuclei in *pam-1* mutant embryos suggested that the SPCC that normally specifies the posterior pole might not be mature or associated with the cortex at the time needed for proper axis specification. We therefore monitored centrosome maturation and position in wild-type and *pam-1(or282)* mutant embryos, using transgenic β-TUBULIN::GFP lines (Fig. 6A-C). When centrosomes first became visible in wild type, they were together and in close association with both the sperm pronucleus and the posterior cortex (*n*=6; Fig. 6A,B,C, part a). In the first few minutes after centrosomes could be detected, they separated from one another and increased in size as they began to nucleate more microtubules (Fig. 6C, parts b,c). During this time, wild-type centrosomes remained in the posterior 25% of the embryo (Fig. 6A-C). By contrast, *pam-1* mutant embryos exhibited multiple defects in centrosome positioning. In all embryos examined, the centrosomes first appeared normally near the presumptive posterior cortex, but then rapidly moved toward the center of the embryo (*n*=13; Fig. 6A,B,C, parts d-f). As a result, the time centrosomes spent near the cortex in *pam-1* mutant embryos was dramatically decreased (Fig. 6A). In addition, in most embryos, this centrosome movement occurred prior to the appearance of the sperm pronucleus, suggesting that centrosome movement occurred during the delayed meiotic exit stage (*n*=10/13). This aberrant centrosome movement was also observed in *pam-1; cyb-3(RNAi)* embryos (*n*=6; data not shown). It is possible that this change in centrosome localization in *pam-1* mutants prevents polarization of the AP axis, through a failure of the centrosomes to influence cortical actomyosin and trigger axis formation.

We next used a combination of DIC and TUBULIN::GFP time-lapse videomicroscopy to track both centrosome-associated microtubules and prouclei at the same time in live embryos. While all *pam-1* embryos showed rapid centrosome movement from the cortex, we observed an additional defect in 32% of *pam-1* mutant embryos (10/31). In these embryos, centrosomes nucleated robust microtubule asters before the appearance of pronuclei. Centrosomes enlarged until they were visible using DIC microscopy and resembled mitotic centrosomes (Fig. 6D, part d). In most cases the enlarged centrosomes diminished in size as the pronuclei became visible (Fig. 6D, part e), but subsequently nucleated more microtubules once again before and during the first mitotic division (*n*=7/10; Fig. 6D, part f). There was no correlation of this premature microtubule nucleation with the subsequent polarity of the division.

Oocyte- or sperm-supplied PAM-1 is sufficient for development

As *pam-1* mutant embryos are defective in events triggered by fertilization, we asked if there might be any paternal contribution of PAM-1 from sperm. We crossed *pam-1(or403)* feminized hermaphrodites and wild-type males, or wild-type feminized hermaphrodites and *pam-1(or403)* males, recorded subsequent hatching rates, and observed early embryonic cell divisions using time-lapse videomicroscopy (Table 4). When *pam-1* feminized hermaphrodites were mated with wild-type males, about 32% of the embryos hatched, a significant increase over *pam-1* mutant hermaphrodite self-progeny hatching rates (1.5%). Furthermore, 25% of embryos observed by DIC optics exhibited early development that was indistinguishable from wild type (3/12), suggesting that paternal PAM-1 is sufficient in some embryos for normal development. The remaining embryos showed phenotypes like those produced by *pam-1* mutant hermaphrodites (*n*=9/12; data not shown). Thus, embryos produced from mutant mothers and wild-type males either appeared normal, or exhibited fully expressed *pam-1* mutant phenotypes. When feminized *pam-1(+)* hermaphrodites were mated to *pam-1(or403)* mutant males, nearly all embryos hatched and exhibited normal early embryonic cell divisions (12/13; data not shown), indicating that maternally supplied PAM-1 is sufficient for embryogenesis. Thus while the paternal contribution can partially rescue *pam-1* mutant oocytes, it is not necessary for wild-type oocytes to develop normally after fertilization.

DISCUSSION

We have shown that the puromycin-sensitive aminopeptidase, PAM-1, is required for meiotic exit and AP axis formation in the one-cell stage *C. elegans* embryo. PAM-1 controls meiotic exit through regulation of the B-type cyclin CYB-3, and appears to control polarity through other target(s). Thus our data implicate protein degradation or processing by PAM-1 in multiple processes. Intriguingly, PAM-1 is supplied both maternally and paternally. The sperm contribution and the coupling of these events through PAM-1 regulation in the one-cell embryo may help to coordinate cell cycle progression and the establishment of AP polarity in the *C. elegans* zygote.

pam-1 encodes a puromycin-sensitive aminopeptidase

PAM-1 is the only *C. elegans* member of the puromycin-sensitive aminopeptidase (PSA) family. This protein is highly conserved, being 36-37% identical to human PSA, with key domains showing higher levels of homology (Brooks et al., 2003). PSA is a member of the M1 class of metalloproteases, which cleave N-terminal amino acids from a variety of substrates (Taylor, 1993). These cleavage events have been implicated in inactivation of neuropeptides in

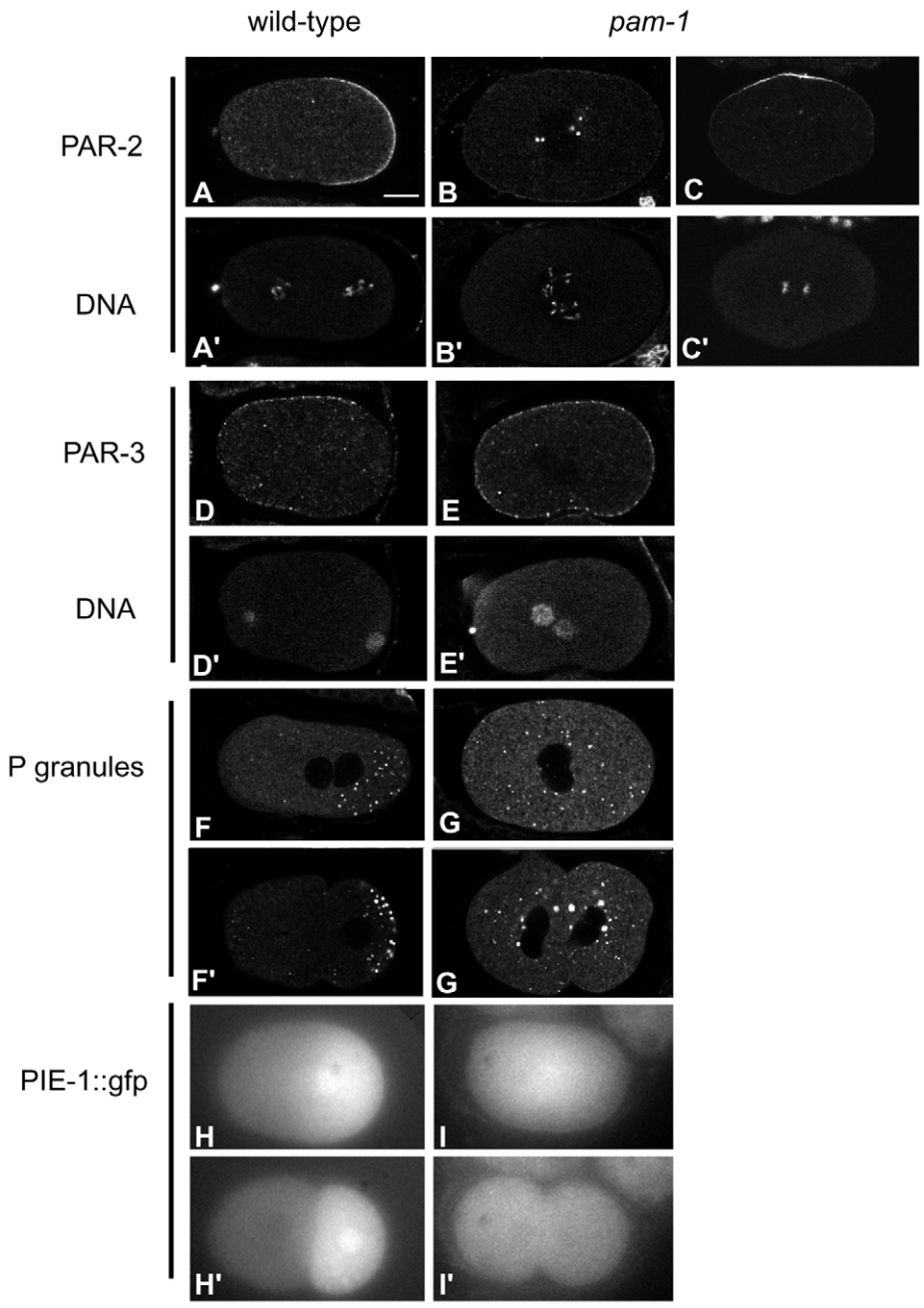

Fig. 4. Polarity markers are disrupted in *pam-1*. (**A-E**) Laser scanning confocal images of PAR-2 and PAR-3 in fixed embryos using indirect immunofluorescence. DNA was stained with TOTO. (A,A′,D,D′) Before and during the first cell division in wild type, PAR-2 localized to the posterior cortex of the embryo and PAR-3 to the anterior cortex. (B,B′) In many one-cell *pam-1* embryos, PAR-2 did not localize to the cortex, but was found instead on cytoplasmic puncta around the pronuclei. (C,C′) When PAR-2 did localize to the cortex, it was often at a lateral position. (E,E′) In roughly half of *pam-1* embryos, PAR-3 localized around the entire periphery. (**F-G′**) PGL-1 antibody staining of the P granules in fixed embryos using indirect immunofluorescence. (**H-I′**) Fluorescent images of PIE-1::GFP taken in living embryos at the one- and two-cell stage. (F,F′) During the one-cell stage in wild type, the germline P granules localized to the posterior pole and were segregated into the posterior daughter cell P_1. (H,H′) Similarly, the transcription factor PIE-1 localized to the posterior and was found in the cytoplasm and nucleus of the P_1 cell. (G,G′) In *pam-1* embryos, the P granules were frequently mislocalized during the first division and often found in both cells at the two-cell stage. (I,I′) PIE-1 failed to become properly partitioned during the first division, and was absent from both daughter cells in embryos that divided symmetrically. Scale bar: 10 μm.

mammalian systems (Hui et al., 1995) and processing of MHC class I peptides (Saric et al., 2001; Stoltze et al., 2000). However, few in vivo substrates are known. This family of proteases include a zinc-binding motif preceded by the GAMEN sequence, which is necessary for protease specificity and enhanced activity (Laustsen et al., 2001). The recessive mutations identified in our alleles affect conserved residues or truncate the protein to reduce or eliminate function. Two mutations affect the GAMEN alanine residue, highlighting its importance.

Loss-of-function studies in mice have implicated PSA in male and female fertility, as well as in growth and pain response (Osada et al., 1999; Osada et al., 2001a; Osada et al., 2001b). Additionally, in *Drosophila*, males with only one wild-type copy of dPSA show reduced fertility (Schulz et al., 2001). In *Arabidopsis*, the single PSA homolog is essential for meiosis (Sanchez-Moran et al., 2004). Less is known about *C. elegans* PSA, although a previous study showed that PAM-1 is expressed in intestinal cells and in neurons of the head, and in the male tail (Brooks et al., 2003). However, this study did not address maternal, paternal or early embryonic expression, due to germline silencing of the transgene reporter (Brooks et al., 2003). The aminopeptidase activity of *C. elegans* PAM-1 is similar to other PSA molecules, except that it is less sensitive to puromycin (Brooks et al., 2003). When RNAi was used to reduce *pam-1* function in adult hermaphrodites, 30% embryonic lethality resulted, although early embryos were not examined (Brooks et al., 2003). We conclude that RNAi does not diminish *pam-1* function as effectively as the mutations we identified, and our studies reveal new roles for this protease in the regulation of meiotic exit and the establishment of the AP body axis.

Table 3. P granule localization in *pam-1* and *pam-1; cyb-3(RNAi)* embryos

Genotype/treatment	*n*	Posterior	Mislocalized	Posterior bias
N2	19	100%	0%	0%
pam-1	24	29.2%	66.6%	4.2%
cyb-3(RNAi)	26	100%	0%	0%
pam-1; cyb-3(RNAi)	36	16.7%	47.2%	36.1%

Shown is the percentage of embryos with PGL-1 staining in each category during first cell division.
Posterior, embryos with all P granules near the posterior pole; mislocalized, embryos with P granules throughout cell; posterior bias, embryos with many P granules toward the posterior pole but significant numbers in other parts of the cell.

A role for PAM-1 in meiotic exit

The most penetrant early defect in *pam-1* mutant embryos was a delayed exit from meiosis II. During meiotic exit in wild-type embryos, the sperm and oocyte chromosomes rapidly decondensed and nuclear envelopes formed, followed by entry into S phase before the first mitosis (Edgar and McGhee, 1988; Vidwans and Su, 2001). In *pam-1* mutant embryos, chromosome decondensation and formation of the pronuclei were delayed after extrusion of the second polar body. Surprisingly, in some *pam-1* mutant embryos, centrosome maturation and microtubule nucleation were not delayed, and thus the centrosomes matured and nucleated large microtubule asters before prouclear formation. Mitotic exit was not delayed in *pam-1* mutants (data not shown), suggesting that the mechanisms governing meiotic and mitotic exit in the early embryo are at least partially distinct. However, PAM-1 might act redundantly with other factors to regulate mitotic exit.

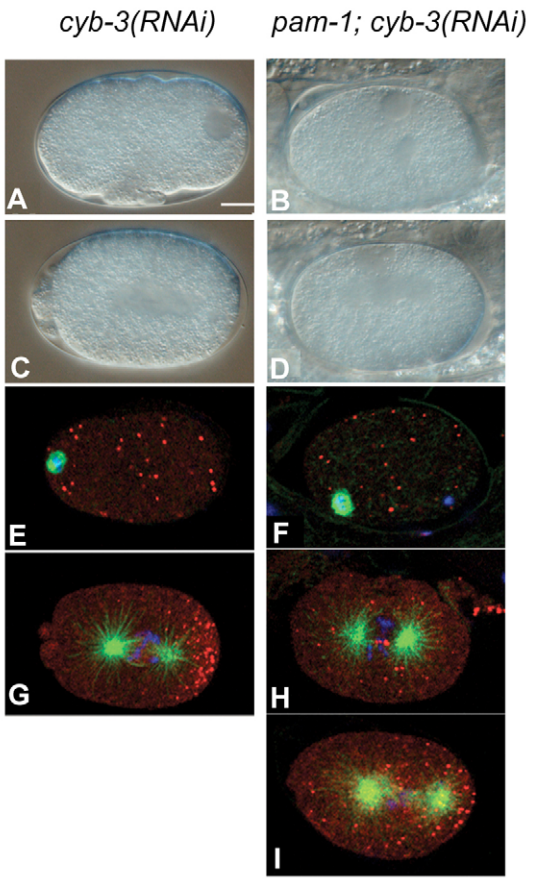

Fig. 5. Polarity defects in *pam-1* mutants occur in the absence of meiotic exit defects. (**A-D**) DIC images of *cyb-3(RNAi)* (A,C) and *pam-1; cyb-3(RNAi)* (B,D) embryos. *cyb-3(RNAi)* embryos show normal pseudocleavage (A) and a posteriorly displaced spindle (C), while many *pam-1; cyb-3(RNAi)* embryos lack pseudocleavage (B) and have a centrally positioned spindle (D). (**E-I**) Triple-stained confocal images with PGL-1 staining of P granules in red, tubulin staining in green and DAPI DNA staining in blue. While P granules were not localized in meiotic embryos of *cyb-3(RNAi)* and *pam-1; cyb-3(RNAi)* (E-F), they were localized to the posterior in all *cyb-3(RNAi)* embryos during the first mitosis (G). P granules failed to localize posteriorly in most *pam-1; cyb-3(RNAi)* embryos, being distributed either throughout the cytoplasm (H) or with a slight but incomplete posterior bias (I). Scale bar: 10 μm.

Ubiquitin-mediated targeting of proteins to the proteasome for degradation is widely used to regulate progression through meiosis and mitosis, and many other processes (reviewed by Bowerman and Kurz, 2006; Deshaies, 1999). Specifically, the APC and cullin-based SCF and ECS E3 ligase complexes are required for progression through meiosis or mitosis in many species. For example, studies in fission yeast have implicated mfr1 as a meiotic-specific activator of the APC necessary to ensure meiotic exit and sporulation following meiosis (Blanco et al., 2001). Similarly, in *C. elegans*, the APC regulates the metaphase to anaphase transition of meiosis I (Golden et al., 2000), and hypomorphic alleles of APC components sometimes exhibit meiotic exit abnormalities (Shakes et al., 2003). Also in *C. elegans*, inactivation of the ubiquitin E3 ligase scaffold, a cullin called CUL-2, or a potential adaptor component for this E3 ligase called ZYG-11, delays the metaphase to anaphase transition during meiosis II, resulting in elevated levels of B-type cyclins and meiotic exit defects (Liu et al., 2004; Sonneville and Gönczy, 2004). Timely meiotic exit is restored in *cul-2* and *zyg-11* mutants when RNAi is used to deplete the B-type cyclins, implicating this E3 ligase in targeting B-type cyclins for degradation and meiotic exit (Liu et al., 2004; Sonneville and Gönczy, 2004).

Our results indicate that the aminopeptidase PAM-1 also acts upstream of CYB-3 to regulate meiotic exit. However, PAM-1 may act more specifically than the known ubiquitin E3 ligases to regulate meiotic exit. Most *pam-1* embryos advance through meiosis normally, with the first defect appearing during meiotic exit. This is in contrast to many ubiquitin E3 ligase mutants, which display more severe meiotic defects. How PAM-1 and ubiquitin-mediated proteolysis interact to influence cell cycle progression and other processes, and whether PAM-1 directly degrades B-type cyclins, are important topics for further study. However, the potential colocalization of PSA, the mammalian PAM-1 homolog, to the 26S proteasome suggests a role downstream of the E3 ligases, perhaps in conjunction with the proteasome (Constam et al., 1995). Studies of a mouse PSA have also implicated these aminopeptidases in mitotic exit (Constam et al., 1995). Thus regulation of cell cycle exit may be a widely conserved role for puromycin-sensitive aminopeptidases.

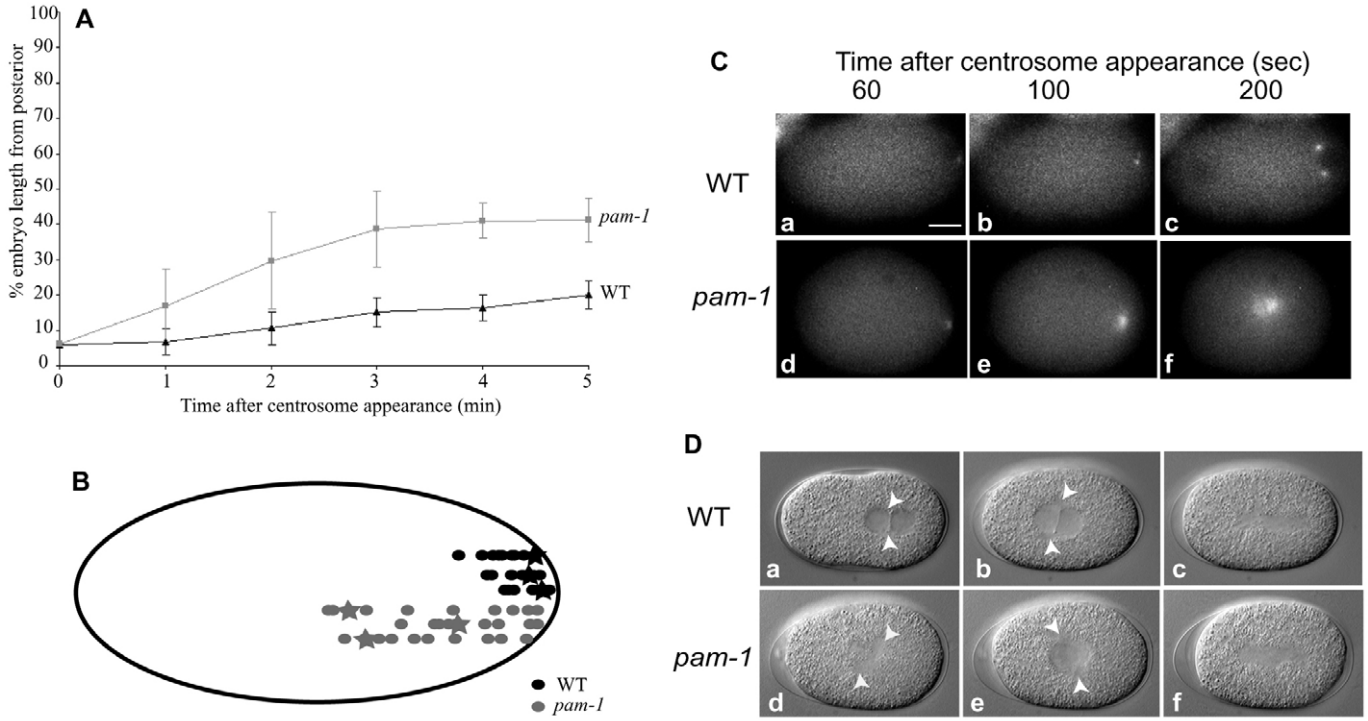

Fig. 6. Aberrant centrosome behavior in *pam-1*. (**A**) Centrosome positions over time, measured from time-lapse images of embryos expressing β-TUBULIN::GFP. Each point represents the average of six wild-type or seven *pam-1* embryos beginning with the moment of the appearance of the centrosomes. In *pam-1* embryos, centrosomes first became visible in the posterior of the embryo, but then quickly moved toward the center of the embryo. (**B**) A plot of centrosome position relative to the posterior pole from three wild-type and three *pam-1* embryos over ten 20 second time points. Each horizontal series represents measurements from one embryo. Measurements were begun when the centrosomes first became visible. Stars indicate the position of the centrosomes when they first separated from one another. The centrosomes in *pam-1* moved quickly toward the center of the embryo. (**C**, parts a-c) Images from a time-lapse β-TUBULIN::GFP movie of a wild-type embryo show movement of the centrosomes over time. By 200 seconds, the centrosomes clearly flanked the sperm pronucleus near the posterior pole of the embryo. (C, parts d-f) In *pam-1* the centrosomes moved quickly into the center of the embryo and remained close together before appearance of the pronuclei. (**D**, parts a-c) By DIC optics, the centrosomes appeared as small dots flanking the pronuclei until the first spindle assembled (white arrowheads). (D, part d) By contrast, in some *pam-1* embryos, the centrosomes began to nucleate microtubules before pronuclear appearance and were visible by DIC optics (white arrowheads). (D, parts e-f) In most cases, the centrosomes reduced in size as the pronuclei formed and then grew larger again as the mitotic spindle assembled. Scale bar: 10 μm.

Polarity defects in *pam*-1 embryos

In addition to exhibiting defects in meiotic exit, *pam-1* embryos fail to polarize the anteroposterior axis. In most *pam-1* mutant embryos, all the earliest AP asymmetries are absent, including cytoplasmic flows, pseudocleavage and asymmetric localization of the PAR proteins. In addition, cytoplasmic determinants such as the P granules and PIE-1 fail to localize, and many embryos divide symmetrically. Thus PAM-1 is important for an early step in axis polarization.

The requirements for PAM-1 during both meiotic exit and establishment of the AP body axis are separable, as depleting CYB-3, a cyclin B, rescues meiotic exit but not the AP axis defects. This analysis of PAM-1 requirements suggests that meiotic exit and polarity establishment are coupled in that they require a common factor, but PAM-1 may target different proteins to regulate these two processes. While we cannot rule out that CYB-3 levels, undetectable in the CYB-3::GFP stain, are still high enough to prevent axis polarization in some *pam-1; cyb-3(RNAi)* embryos, we favor a model in which PAM-1 targets CYB-3 to regulate meiotic exit and an additional factor to regulate centrosome movements in the embryo to influence polarity. While other studies have suggested a role of E3 ligases in both meiosis and polarity (Liu et al., 2004; Rappleye et al., 2002; Sonneville and Gönczy, 2004), our results provide an additional link between AP axis formation and proteolytic regulation.

PAM-1 may regulate polarity through centrosome association with the cortex

Around the time of meiotic exit, the sperm-donated centrosome duplicates, matures and nucleates microtubules (O'Connell, 2000). Both proper maturation of the centrosome (Hamill et al., 2002; O'Connell et al., 2000) and a close SPCC association with the posterior cortex (Cowan and Hyman, 2004b; Rappleye et al., 2002) are required for axis formation. Centrosomes mature and microtubule asters form in *pam-1* mutants. However, both the sperm chromosomes and the centrosomes move away from the cortex prematurely, during the meiotic exit delay. Thus the lack of axis polarization in *pam-1* mutants may result from the absence of close centrosome association with the cortex. Current models suggest that the SPCC centrosomes downregulate cortical microfilament contractility, resulting in cortical flows and a movement of PAR-3 away from the SPCC, to form an anterior pole opposite the site of the SPCC (Cuenca et al., 2003; Jenkins et al., 2006; Munro et al., 2004). As the centrosome moves quickly away from the cortex in *pam-1* mutants, it may fail to induce

Table 4. Maternal and paternal contributions to *pam-1* embryonic lethality at 25°C

Hermaphrodite		*n*	% Embryos hatching
pam-1		407	1.5%
pam-1/dpy-13 unc-24		428	99.3%
Female	**Male**	***n***	**% Embryos hatching**
fog-2	*N2*	605	99.7%
fog-2	*pam-1*	2161	94.3%*
fog-2; pam-1	*N2*	198	32.3%

All scoring done with *pam-1(or403)*.
n, number of embryos examined from each cross.
fog-2 is a feminized strain (Schedl and Kimble, 1988).
*No significant difference by Student's *t*-test when compared with control cross of *fog-2* females and N2 males.

the cortical changes. This hypothesis is consistent with the lack of posterior PAR-2 localization, and the presence of PAR-3 throughout the entire cortex, in most *pam-1* mutant embryos.

Paternal contribution of PAM-1

The *pam-1* gene product is contributed to the zygote by both the sperm and the egg. Egg contribution is necessary in nearly all embryos for viability and is also fully sufficient for normal development. By contrast, the sperm contribution of PAM-1 is not necessary for embryo viability but is sufficient in many cases. It is unlikely that the rescue *of pam-1* mutant oocytes by wild-type sperm is due to zygotic expression of *pam-1*, as the rescued processes occur shortly after fertilization, before the zygotic genome is activated (Seydoux and Fire, 1994). Thus PAM-1 is partially contributed as a paternal gene product, although this contribution appears nonessential. It is interesting to note that, although cues from the sperm are known to promote resumption of meiosis and axis polarization, only one true paternal-effect mutation, *spe-11*, has been identified to date in *C. elegans* (Browning and Strome, 1996). Despite this, many mutants that affect early development of the embryo, including *pam-1*, show both maternal and paternal contributions of the gene product (Gönczy et al., 1999; Lee et al., 2001; O'Connell et al., 1998). Perhaps the addition of multiple sperm-contributed proteins at fertilization helps to produce a threshold concentration of factors necessary for the progression into embryogenesis.

Possible mechanisms for PAM-1 action

While in vivo substrates of puromycin-sensitive aminopeptidases are poorly understood, these enzymes have been implicated in a variety of processes, including neuropeptide inactivation (Hui et al., 1995), MHC class I peptide processing (Saric et al., 2001; Stoltze et al., 2000) and cell cycle regulation in conjunction with the proteasome (Constam et al., 1995). The role of PAM-1 role in the early embryo may be complex, causing the activation of some peptides through N-terminal trimming and the degradation of other proteins, perhaps in conjunction with the proteasome. One intriguing possibility is that PAM-1 may trigger peptides for degradation through the N-end rule, with removal of N-terminal residues by PAM-1 exposing amino acids that target the protein for ubiquitin-mediated proteolysis (Varshavsky, 1996).

Our study provides new insights into the PAM-1 aminopeptidase and its roles in early development. Because PAM-1 is a member of the highly conserved PSA gene family, its role in cell cycle progression and cell polarity may provide important new insights into these processes in other systems.

We thank K. Kemphues and S. Strome for antibodies, P. Gönczy, G. Seydoux, C. Malone and J. Austin for GFP strains. Other strains were supplied by the *C. elegans* Genetics Center, which is funded by the NIH National Center for Research Resources. We also thank C. Trzepacz for sharing data prior to publication. R.L. was supported by a postdoctoral grant from the American Cancer Society (PF-00-097-010-MBC), an NIH-AREA grant (1 R15 GM72523-01) and institutional grants from Ursinus College (HHMI and VanSant). M.M. was supported in part by a Merck-SURF grant, and B.B. by R01-GM49869 from the NIH.

References

Albertson, D. G. (1984). Formation of the first cleavage spindle in nematode embryos. *Dev. Biol.* **101**, 61-72.
Albertson, D. G. and Thomson, J. N. (1993). Segregation of holocentric chromosomes at meiosis in the nematode, Caenorhabditis elegans. *Chromosome Res.* **1**, 15-26.
Blanco, M. A., Pelloquin, L. and Moreno, S. (2001). Fission yeast mfr1 activates APC and coordinates meiotic nuclear division with sporulation. *J. Cell Sci.* **114**, 2135-2143.
Bowerman, B. and Kurz, T. (2006). Degrade to create: developmental requirements for ubiquitin-mediated proteolysis during early *C. elegans* embryogenesis. *Development* **133**, 773-784.
Brenner, S. (1974). The genetics of Caenorhabditis elegans. *Genetics* **77**, 71-94.
Brooks, D. R., Hooper, N. M. and Isaac, R. E. (2003). The Caenorhabditis elegans orthologue of mammalian puromycin-sensitive aminopeptidase has roles in embryogenesis and reproduction. *J. Biol. Chem.* **278**, 42795-42801.
Browning, H. and Strome, S. (1996). A sperm-supplied factor required for embryogenesis in C. elegans. *Development* **122**, 391-404.
Constam, D. B., Tobler, A. R., Rensing-Ehl, A., Kemler, I., Hersh, L. B. and Fontana, A. (1995). Puromycin-sensitive aminopeptidase. Sequence analysis, expression, and functional characterization. *J. Biol. Chem.* **270**, 26931-26939.
Cowan, C. R. and Hyman, A. A. (2004a). Asymmetric cell division in C. elegans: cortical polarity and spindle positioning. *Annu. Rev. Cell Dev. Biol.* **20**, 427-453.
Cowan, C. R. and Hyman, A. A. (2004b). Centrosomes direct cell polarity independently of microtubule assembly in C. elegans embryos. *Nature* **431**, 92-96.
Cuenca, A. A., Schetter, A., Aceto, D., Kemphues, K. and Seydoux, G. (2003). Polarization of the C. elegans zygote proceeds via distinct establishment and maintenance phases. *Development* **130**, 1255-1265.
DeRenzo, C., Reese, K. J. and Seydoux, G. (2003). Exclusion of germ plasm proteins from somatic lineages by cullin-dependent degradation. *Nature* **424**, 685-689.
Deshaies, R. J. (1999). SCF and Cullin/Ring H2-based ubiquitin ligases. *Annu. Rev. Cell Dev. Biol.* **15**, 435-467.
Edgar, L. G. and McGhee, J. D. (1988). DNA synthesis and the control of embryonic gene expression in C. elegans. *Cell* **53**, 589-599.
Encalada, S. E., Martin, P. R., Phillips, J. B., Lyczak, R., Hamill, D. R., Swan, K. A. and Bowerman, B. (2000). DNA replication defects delay cell division and disrupt cell polarity in early Caenorhabditis elegans embryos. *Dev. Biol.* **228**, 225-238.
Golden, A., Sadler, P. L., Wallenfang, M. R., Schumacher, J. M., Hamill, D. R., Bates, G., Bowerman, B., Seydoux, G. and Shakes, D. C. (2000). Metaphase to anaphase (mat) transition-defective mutants in Caenorhabditis elegans. *J. Cell Biol.* **151**, 1469-1482.
Goldstein, B. and Hird, S. N. (1996). Specification of the anteroposterior axis in Caenorhabditis elegans. *Development* **122**, 1467-1474.
Gönczy, P., Schnabel, H., Kaletta, T., Amores, A. D., Hyman, T. and Schnabel, R. (1999). Dissection of cell division processes in the one cell stage Caenorhabditis elegans embryo by mutational analysis. *J. Cell Biol.* **144**, 927-946.
Greenstein, D. (2005). Control of oocyte meiotic maturation and fertilization. In *WormBook* (ed. The C. *elegans* Research Community), pp. 1-23. doi/10.1895/wormbook.1.53.1, http://www.wormbook.org.
Hamill, D. R., Severson, A. F., Carter, J. C. and Bowerman, B. (2002). Centrosome maturation and mitotic spindle assembly in C. elegans require SPD-5, a protein with multiple coiled-coil domains. *Dev. Cell* **3**, 673-684.
Hird, S. N., Paulsen, J. E. and Strome, S. (1996). Segregation of germ granules

in living Caenorhabditis elegans embryos: cell-type-specific mechanisms for cytoplasmic localisation. *Development* **122**, 1303-1312.
Hui, M., Budai, E. D., Lajtha, A., Palkovits, M. and Hui, K. S. (1995). Changes in puromycin-sensitive aminopeptidases in postmortem schizophrenic brain regions. *Neurochem. Int.* **27**, 433-441.
Hyman, A. A. and White, J. G. (1987). Determination of cell division axes in the early embryogenesis of Caenorhabditis elegans. *J. Cell Biol.* **105**, 2123-2135.
Jenkins, N., Saam, J. R. and Mango, S. E. (2006). CYK-4/GAP provides a localized cue to initiate anteroposterior polarity upon fertilization. *Science* **313**, 1298-1301.
Kamath, R. S., Fraser, A. G., Dong, Y., Poulin, G., Durbin, R., Gotta, M., Kanapin, A., Le Bot, N., Moreno, S., Sohrmann, M. et al. (2003). Systematic functional analysis of the Caenorhabditis elegans genome using RNAi. *Nature* **421**, 231-237.
Koepp, D. M., Harper, J. W. and Elledge, S. J. (1999). How the cyclin became a cyclin: regulated proteolysis in the cell cycle. *Cell* **97**, 431-434.
Laustsen, P. G., Vang, S. and Kristensen, T. (2001). Mutational analysis of the active site of human insulin-regulated aminopeptidase. *Eur. J. Biochem.* **268**, 98-104.
Lee, J., Jee, C., Lee, J. I., Lee, M. H., Koo, H. S., Chung, C. H. and Ahnn, J. (2001). A deubiquitinating enzyme, UCH/CeUBP130, has an essential role in the formation of a functional microtubule-organizing centre (MTOC) during early cleavage in C. elegans. *Genes Cells* **6**, 899-911.
Liu, J., Vasudevan, S. and Kipreos, E. T. (2004). CUL-2 and ZYG-11 promote meiotic anaphase II and the proper placement of the anterior-posterior axis in C. elegans. *Development* **131**, 3513-3525.
Lyczak, R., Gomes, J. E. and Bowerman, B. (2002). Heads or tails: cell polarity and axis formation in the early Caenorhabditis elegans embryo. *Dev. Cell* **3**, 157-166.
McCarter, J., Bartlett, B., Dang, T. and Schedl, T. (1999). On the control of oocyte meiotic maturation and ovulation in Caenorhabditis elegans. *Dev. Biol.* **205**, 111-128.
McNally, K. L. and McNally, F. J. (2005). Fertilization initiates the transition from anaphase I to metaphase II during female meiosis in C. elegans. *Dev. Biol.* **282**, 218-230.
Munro, E., Nance, J. and Priess, J. R. (2004). Cortical flows powered by asymmetrical contraction transport PAR proteins to establish and maintain anterior-posterior polarity in the early C. elegans embryo. *Dev. Cell* **7**, 413-424.
O'Connell, K. F. (2000). The centrosome of the early C. elegans embryo: inheritance, assembly, replication, and developmental roles. *Curr. Top. Dev. Biol.* **49**, 365-384.
O'Connell, K. F., Leys, C. M. and White, J. G. (1998). A genetic screen for temperature-sensitive cell-division mutants of Caenorhabditis elegans. *Genetics* **149**, 1303-1321.
O'Connell, K. F., Maxwell, K. N. and White, J. G. (2000). The spd-2 gene is required for polarization of the anteroposterior axis and formation of the sperm asters in the Caenorhabditis elegans zygote. *Dev. Biol.* **222**, 55-70.
Osada, T., Ikegami, S., Takiguchi-Hayashi, K., Yamazaki, Y., Katoh-Fukui, Y., Higashinakagawa, T., Sakaki, Y. and Takeuchi, T. (1999). Increased anxiety and impaired pain response in puromycin-sensitive aminopeptidase gene-deficient mice obtained by a mouse gene-trap method. *J. Neurosci.* **19**, 6068-6078.
Osada, T., Watanabe, G., Kondo, S., Toyoda, M., Sakaki, Y. and Takeuchi, T. (2001a). Male reproductive defects caused by puromycin-sensitive aminopeptidase deficiency in mice. *Mol. Endocrinol.* **15**, 960-971.
Osada, T., Watanabe, G., Sakaki, Y. and Takeuchi, T. (2001b). Puromycin-sensitive aminopeptidase is essential for the maternal recognition of pregnancy in mice. *Mol. Endocrinol.* **15**, 882-893.
Praitis, V., Casey, E., Collar, D. and Austin, J. (2001). Creation of low-copy integrated transgenic lines in Caenorhabditis elegans. *Genetics* **157**, 1217-1226.
Rappleye, C. A., Tagawa, A., Lyczak, R., Bowerman, B. and Aroian, R. V. (2002). The anaphase-promoting complex and separin are required for embryonic anterior-posterior axis formation. *Dev. Cell* **2**, 195-206.
Reese, K. J., Dunn, M. A., Waddle, J. A. and Seydoux, G. (2000). Asymmetric segregation of PIE-1 in C. elegans is mediated by two complementary mechanisms that act through separate PIE-1 protein domains. *Mol. Cell* **6**, 445-455.
Rose, L. S. and Kemphues, K. J. (1998). Early patterning of the C. elegans embryo. *Annu. Rev. Genet.* **32**, 521-545.
Sadler, P. L. and Shakes, D. C. (2000). Anucleate Caenorhabditis elegans sperm can crawl, fertilize oocytes and direct anterior-posterior polarization of the 1-cell embryo. *Development* **127**, 355-366.
Sanchez-Moran, E., Jones, G. H., Franklin, F. C. and Santos, J. L. (2004). A puromycin-sensitive aminopeptidase is essential for meiosis in Arabidopsis thaliana. *Plant Cell* **16**, 2895-2909.
Saric, T., Beninga, J., Graef, C. I., Akopian, T. N., Rock, K. L. and Goldberg, A. L. (2001). Major histocompatibility complex class I-presented antigenic peptides are degraded in cytosolic extracts primarily by thimet oligopeptidase. *J. Biol. Chem.* **276**, 36474-36481.
Schedl, T. and Kimble, J. (1988). fog-2, a germ-line-specific sex determination gene required for hermaphrodite spermatogenesis in Caenorhabditis elegans. *Genetics* **119**, 43-61.
Schneider, S. Q. and Bowerman, B. (2003). Cell polarity and the cytoskeleton in the Caenorhabditis elegans zygote. *Annu. Rev. Genet.* **37**, 221-249.
Schulz, C., Perezgasga, L. and Fuller, M. T. (2001). Genetic analysis of dPsa, the Drosophila orthologue of puromycin-sensitive aminopeptidase, suggests redundancy of aminopeptidases. *Dev. Genes Evol.* **211**, 581-588.
Severson, A. F., Baillie, D. L. and Bowerman, B. (2002). A formin homology protein and a profilin are required for cytokinesis and Arp2/3-independent assembly of cortical microfilaments in C. elegans. *Curr. Biol.* **12**, 2066-2075.
Seydoux, G. and Fire, A. (1994). Soma-germline asymmetry in the distributions of embryonic RNAs in Caenorhabditis elegans. *Development* **120**, 2823-2834.
Shakes, D. C., Sadler, P. L., Schumacher, J. M., Abdolrasulnia, M. and Golden, A. (2003). Developmental defects observed in hypomorphic anaphase-promoting complex mutants are linked to cell cycle abnormalities. *Development* **130**, 1605-1620.
Sonneville, R. and Gönczy, P. (2004). Zyg-11 and cul-2 regulate progression through meiosis II and polarity establishment in C. elegans. *Development* **131**, 3527-3543.
Stoltze, L., Schirle, M., Schwarz, G., Schroter, C., Thompson, M. W., Hersh, L. B., Kalbacher, H., Stevanovic, S., Rammensee, H. G. and Schild, H. (2000). Two new proteases in the MHC class I processing pathway. *Nat. Immunol.* **1**, 413-418.
Strome, S. and Wood, W. B. (1982). Immunofluorescence visualization of germ-line-specific cytoplasmic granules in embryos, larvae, and adults of Caenorhabditis elegans. *Proc. Natl. Acad. Sci. USA* **79**, 1558-1562.
Strome, S., Powers, J., Dunn, M., Reese, K., Malone, C. J., White, J., Seydoux, G. and Saxton, W. (2001). Spindle dynamics and the role of gamma-tubulin in early Caenorhabditis elegans embryos. *Mol. Biol. Cell* **12**, 1751-1764.
Sulston, J. E., Schierenberg, E., White, J. G. and Thomson, J. N. (1983). The embryonic cell lineage of the nematode Caenorhabditis elegans. *Dev. Biol.* **100**, 64-119.
Taylor, A. (1993). Aminopeptidases: structure and function. *FASEB J.* **7**, 290-298.
Varshavsky, A. (1996). The N-end rule: functions, mysteries, uses. *Proc. Natl. Acad. Sci. USA* **93**, 12142-12149.
Vidwans, S. J. and Su, T. T. (2001). Cycling through development in Drosophila and other metazoa. *Nat. Cell Biol.* **3**, E35-E39.
Wicks, S. R., Yeh, R. T., Gish, W. R., Waterston, R. H. and Plasterk, R. H. (2001). Rapid gene mapping in Caenorhabditis elegans using a high density polymorphism map. *Nat. Genet.* **28**, 160-164.